# Stabilization of all-aqueous droplets by interfacial self-assembly of fatty acids bilayers

Noëmie Coudon, Laurence Navailles, Frédéric Nallet, Isabelle Ly, Ahmed Bentaleb, Jean-Paul Chapel, Laure Beven, Jean-Paul Douliez, Nicolas Martin

# Stabilization of all-aqueous droplets by interfacial self-assembly of fatty acids bilayers

Noëmie Coudon,[1] Laurence Navailles,[1] Frédéric Nallet,[1] Isabelle Ly,[1] Ahmed Bentaleb,[1] Jean-Paul Chapel,[1] Laure Béven,[2] Jean-Paul Douliez[2*] and Nicolas Martin[1*]

1 Univ. Bordeaux, CNRS, Centre de recherche Paul-Pascal, UMR 5031, 115 Avenue du Dr. Schweitzer, 33600 Pessac, France

2 Univ. Bordeaux, INRAE, Biologie du Fruit et Pathologie, UMR 1332, 71 Avenue Edouard Bourlaux, 33140 Villenave d'Ornon, France

* nicolas.martin@crpp.cnrs.fr; jean-paul.douliez@inrae.fr

**"This is the accepted version of the following article:** N. Coudon**,** L. Navailles, F. Nallet, I. Ly, A. Bentaleb, J.-P. Chapel, L. Béven, J.-P. Douliez, N. Martin, *J. Colloid Int. Sci.*, **2022**, *617*, 257-266**, which has been published in final form at** https://doi.org/10.1016/j.jcis.2022.02.138 © 2022 Elsevier**."**

## Abstract

All-aqueous microdroplets produced by liquid-liquid phase separation have emerged as promising models of artificial cells, and offer new approaches for the solvent-free encapsulation of fragile solutes. Yet, the lack of a membrane on such droplets makes them intrinsically unstable against coarsening, and precludes a fine control over chemical localization, as solutes can freely diffuse through the interface. Herein, we report the construction of stable and impermeable water-in-water emulsions via the interfacial self-assembly of mixed sodium oleate/1-decanol bilayers on dextran-rich droplets produced by segregative liquid-liquid phase separation with poly(ethylene glycol). Lipids spontaneously self-assemble as multilamellar structures at the surface of the droplets as revealed by freeze-fracture transmission electron microscopy and small-angle X-ray scattering. We further demonstrate that the lipid-based membrane is impermeable to oligonucleotides and proteins, but also to a low molecular weight dye, so that a strict chemical encapsulation can be achieved by spontaneous partitioning within the droplets before membrane self-assembly. Taken together, our results highlight the ease of production of fatty acid-stabilized all-aqueous emulsions droplets able to encapsulate a range of solutes without the need of oil or organic solvents, paving the way to the construction of robust membrane-bounded, polymer-rich artificial cells.

*liquid-liquid phase separation ● water-in-water emulsion ● fatty acids ● interfacial self-assembly ● artificial cells*

## Introduction

Liquid-liquid phase separation (LLPS) in dilute aqueous polymer solutions produces chemically-enriched microdroplets that have emerged in recent years as promising compartments to assemble rudimentary forms of artificial cells.[1 2 3 4] Examples of such all-aqueous droplets include complex coacervates produced by associative LLPS between oppositely charged polyelectrolytes[5] or surfactants,[6 7 8] but also polymer-rich droplets formed by segregative LLPS between poly(ethylene glycol) (PEG) and dextran (conventionally referred to as "aqueous two-phase systems", or ATPS).[1 9] Due to their differential chemical composition and physical properties compared to the continuous phase, these crowded droplets spontaneously and selectively accumulate various solutes,[5 6 10] including molecular dyes,[5 6] proteins[1] or polynucleotides.[11] The typical concentrations of guest solutes within droplets are significantly higher than that in the continuous phase,[5 6] which provides a simple mechanism to localize and concentrate functional species.

Due to the absence of a physical membrane, all-aqueous droplets produced by LLPS yet suffer from two main limitations: (i) the material sequestered in the droplets is in dynamic equilibrium with the environment and may exchange with the continuous phase and adjacent droplets via passive diffusion;[12] and (ii) these microdroplets are thermodynamically unstable and undergo macroscopic phase separation over time, mostly due to the gradual coalescence of smaller droplets into larger ones, together with Ostwald ripening. By analogy with conventional water/oil two-phase systems, all-aqueous droplets suspensions have thus been described as 'water-in-water' (W/W) emulsions.[13] Stabilization of these all-aqueous emulsions is yet far from trivial due to the ultra-low surface tension (~ 0.1-100 μN $m^{-1}$, ref [14]) and associated large thickness (~ tens of nm[15 16]) of the water/water interface. Strategies to stabilize all-aqueous droplets have therefore essentially relied on the use of large objects, typically of a size commensurate to that of the water/water interface, to produce Pickering-like W/W emulsions.[17 18 19] Examples of stabilizers include polymer-based nano- or microparticles[17 19 20 21 22] and microgels,[23] cellulose nanocrystals,[24] nanoplates,[15] protein clusters[25] and fibrils,[26] lipid nanocapsules[27] or small unilamellar vesicles.[28] While these approaches are effective in stabilizing all-aqueous droplets against macroscopic phase separation, they produce highly permeable shells due to the large interstitial pores formed in between the adsorbed objects, so that low molecular weight molecules, but also larger species such as oligonucleotides, can still freely diffuse in and out of the droplets.[28]

Recently, alternative stabilization approaches using amphiphiles have emerged to build more biologically-relevant, cell-mimetic membranes, and restrict the diffusion of biomolecules across the water/water interface. For instance, rationally designed block copolymers with a differential affinity for the two aqueous phases have been shown to self-assemble at both complex coacervate[29] and PEG/dextran[30] interfaces to produce a continuous monolayer preventing droplet coalescence. Other studies have reported the self-assembly of fatty acid[31] or phospholipid[32 33] multilayers around complex coacervate droplets, together with the interfacial assembly of phospholipids on dextran-rich droplets suspended in PEG.[34] In all these systems, the produced membranes were yet still permeable to small molecules[29 31 32 33] and, in some cases, also to larger biomolecules such as oligonucleotides.[33] In addition, careful polymer design and synthesis, or specific formulation pathways (gradual addition of fatty acids and pH variation,[31] dry film rehydration,[33 34] or cooling/resting steps[32]) were required to obtain membrane-coated polymer-crowded droplets. To the best of our knowledge, single-chain amphiphiles have never been shown to stabilize droplets produced by segregative liquid-liquid phase separation.

Here, we show that admixtures of a fatty acid and a fatty alcohol readily produce impermeable bilayers on PEG/dextran droplets via spontaneous interfacial self-assembly. Our bulk formulation approach is very simple and highly robust as it only relies on the stepwise addition of sodium oleate and 1-decanol (**Supplementary Figure 1**) to a suspension of dextran-in-PEG droplets under vigorous

shaking to instantaneously produce uniformly-sized, bilayer-coated micro-droplets. Strikingly, the resulting W/W emulsion remains stable for several weeks and can be centrifuged at moderated speed without loss of integrity, which suggests that a robust elastic shell is formed around the droplets. We systematically investigate the influence of the concentrations of sodium oleate and 1-decanol on the size and stability of the emulsion droplets to gain insight into the interfacial amphiphile self-assembly. By combining freeze-fracture transmission electron microscopy and small-angle X-ray scattering, we further show that the membranous shell is composed of multiple sodium oleate/1-decanol bilayers interspaced by a large water layer. We last demonstrate that this multilayer architecture prevents diffusion of biomacromolecules but also of a low molecular weight dye, confirming that a highly impermeable shell is produced. Overall, our simple self-assembly strategy offers a new approach for the stabilization of all-aqueous droplets able to encapsulate biologically relevant solutes, paving the way to the construction of biomimetic functional cell-like structures and greener, solvent-free compartments.

## Experimental section

### Materials

The following chemicals were purchased from Sigma-Aldrich and used as received: dextran 500 kg/mol, poly(ethylene glycol) 20 kg/mol (PEG), sodium oleate, 1-decanol, double-stranded DNA (low molecular weight from salmon sperm, *ds*DNA), Nile Red, rhodamine isothiocyanate (RITC), fluorescein isothiocyanate-dextran 500 kg/mol (FITC-dextran), calcein, bovine serum albumin (BSA), pyrene, dimethylsulfoxide (DMSO), ethanol and hydrochloric acid. SYBR Green I was purchased from Thermofisher. Milli-Q-purified water was used for all experiments.

### Preparation of stock solutions

A PEG/dextran stock mixture (70 mg/mL PEG, 42.5 mg/mL dextran) was prepared by dissolving 2.8 g of PEG and 1.7 g of dextran in 40 mL of Milli-Q water in a glass container, and mixed under magnetic stirring for 24 hours at room temperature to ensure complete dissolution of the polymers. This stock solution was stored at 4°C. A 50 mg/mL (164 mM) stock solution of sodium oleate was prepared by dispersing an appropriate amount of solid sodium oleate powder in Milli-Q water, followed by stirring and heating to 60°C until the solid fully dissolved. A 1 mM Nile Red stock solution was prepared by dissolving an appropriate amount of solid dye in DMSO, then a small aliquot of this solution was added to the sodium oleate stock solution (40 µM final Nile Red concentration). A 40 µM stock solution of FITC-dextran was prepared by dissolving a given amount of the polymer in Milli-Q water. A 1 mL SYBR-*ds*DNA stock solution was prepared by dissolving *ds*DNA in Milli-Q water (100 mM final *ds*DNA concentration), then adding 0.5 µL of SYBR Green I commercial stock solution. The solution was then diluted to 0.5 mM (*ds*DNA concentration) for use. Stock solutions of RITC-BSA and calcein were prepared at a concentration of 7.6 µM and 100 µM, respectively, by dissolving the freeze-dried protein (see below) or dye powder in Milli-Q water. All these solutions were aliquoted and stored at -20°C until use.

### Preparation of all-aqueous emulsions

To prepare uncoated dextran-in-PEG droplets, 5 µL of FITC-dextran stock solution were added to 2 mL of the stock PEG/dextran solution in an Eppendorf tube and mixed thoroughly by vortexing (final FITC-dextran concentration of 100 nM). To prepare all-aqueous droplets in the presence of amphiphiles, a given volume of Nile Red-doped sodium oleate stock solution was added dropwise to 2 mL of FITC-dextran-doped PEG/dextran mixture in an Eppendorf tube under vortexing, followed by the dropwise addition of a given volume of pure 1-decanol under vortexing. Alternatively, the addition of 1-decanol

was replaced by the dropwise addition of a small amount of 1 M HCl to decrease the pH to ~9. The pH of each final emulsions was measured using a calibrated pH-metre equipped with a micro-electrode.

**Bulk stability of all-aqueous droplets**

Bulk stability of dextran-in-PEG droplets was studied in the presence or absence of amphiphiles by turbidity measurements and confocal fluorescence microscopy observations. Experiments were performed both at $t = 0$ (i.e. immediately after vortexing) and after 24 hours of resting in a tube without shaking.

Confocal fluorescence microscopy images were acquired on a Leica SP2 confocal laser scanning microscope attached to a Leica DMI RE2 inverted microscope using a ×63 oil immersion lens (HCX PL APO, 1.4 NA). Typically, 10 µL of solution were loaded into a home-made capillary chamber assembled with a UV-curing glue, and droplets were left to settle for 5 minutes before imaging. Images were processed using ImageJ. Dyes were excited by using the following excitation ($\lambda_{ex}$) and emission wavelength range ($\lambda_{em}$): FITC-dextran, $\lambda_{ex}$ = 488 nm, $\lambda_{em}$ = 495-565 nm; Nile Red, $\lambda_{ex}$ = 561 nm, $\lambda_{em}$ = 630-760 nm.

Turbidity measurements on the different emulsion samples were also acquired at t = 0 (i.e. just after formulation and vortexing) and after 24 hours or longer of resting without shaking in a plastic cuvette. Measurements were performed at 700 nm on a Cary 100 UV-vis spectrophotometer blanked to a pure PEG-rich phase. Experiments were repeated three times. The percent turbidity was calculated as $(1\text{-}10^{-A}) \times 100$, where A is the absorbance measured at 700 nm.

**Construction of the partial phase diagram: droplet size analysis**

To build the partial phase diagram, emulsion droplets prepared at varying sodium oleate and 1-decanol concentrations were imaged by optical microscopy just after formulation ($t = 0$) and after 24 hours of resting in a tube ($t$ = 24h) using a Leica DMI 4000B inverted microscope. The size of 50 droplets from 5 different fields of view of the same sample was measured using ImageJ, and the average value and standard deviation determined.

**Freeze-Fracture Transmission Electron Microscopy**

Dextran-in-PEG droplets coated with sodium oleate (5 mM) and 1-decanol (15 mM) were prepared as described above. Freeze-fracture replica preparation was performed by first depositing a drop of the sample on a gold capsule and then freezing it by quickly plunging the holder into liquid propane at the temperature of liquid nitrogen. Frozen samples were inserted inside a Leica BAF060 freeze fracture apparatus, then were fractured with a blade at a temperature of -150°C and a pressure of $9.10^{-7}$ mbar. The freshly fractured surface was shadowed by the deposition of platinum at an angle of 45°, and the replica was reinforced by carbon deposition at an angle of 90°. Outside the apparatus, the samples were dissolved in chloroform/ethanol. The detached replicas were rinsed several times with chloroform/ethanol, then pure ethanol and finally water. The replicas were finally collected on 400 mesh copper grids and dried before TEM imaging. Transmission electron microscopy (TEM) was performed using a Hitachi H600 TEM at 75 kV.

**Small-angle X-ray scattering**

Small-angle X-ray scattering (SAXS) experiments were carried out on a XEUSS 2.0 device (XENOCS, Grenoble, France). Coupled to a FOX$^{3D}$ single reflection optical mirror centred on the Cu $K_\alpha$ radiation ($\lambda$ = 1.54 Å), the GeniX$^{3D}$ source delivers a 8 keV beam which is further collimated by a set of 2 motorized scatter-less (4-blade) slits. The dispersion of stabilized dextran-in-PEG droplets (PEG 70 mg/mL; dextran 42.5 mg/mL; sodium oleate 5 mM and 1-decanol 15 mM) was loaded in thin quartz capillaries (optical path 1.5mm, WJM-Glas/Müller GmbH, Germany) and the signal collected for 3 hours. The images were collected on a two-dimensional PILATUS-300k detector (DECTRIS, Baden-Dättwill,

Switzerland) placed perpendicularly to the direct beam at distances of 1.63m or 2.47m, calibrated in both cases with a Silver Behenate standard. Even though the XEUSS 2.0 device offers a wholly evacuated flight path from the downstream end of the mirror to a few centimetres before the detector, including the samples, properly subtracting the direct beam wings is difficult. This results in lower limits in the accessible scattering wave vector q-range, namely 0.01 $Å^{-1}$ and 0.003 $Å^{-1}$, respectively, for the two configurations. Close to the upper limits in q-range, about 0.24 $Å^{-1}$ and 0.16 $Å^{-1}$, respectively, background contributions (cosmic rays) may become significant. This is particularly true for the 2.47m configuration, where the combination of a tight collimation, a large sample-to-detector distance and an intrinsically low scattering power of the irradiated sample lead to a small signal buried in noise.

The 1D diffractograms (intensity *I* vs *q*) were obtained by processing the raw detector images with the FOXTROT software (collaboration between XENOCS and the SOLEIL synchrotron (Gif-sur-Yvette, FRANCE) SWING beamline team), subtracting empty beam when appropriate (1.63m configuration). A further signal processing was necessary for the 2.47m configuration: the background contribution was estimated by assuming an overall $1/q^2$ decay for the signal of the sample, as expected for flat bilayers in the intermediate scattering range. The fitted baseline was then subtracted from the data, evidencing the first order Bragg peak of the multilamellar stack of bilayers at quite a small scattering wave vector $q_0$ (inset in Figure 4B). Note that for such a small value of $q_0$, the higher-intensity, lower-resolution 1.63m configuration is not appropriate owing to the spurious signal of the direct beam wings.

**Preparation of fluorescently-labelled protein.**

A BSA solution (4 mg/mL) was prepared by dissolving the freeze-dried protein powder in 1 mL of 0.5 M carbonate buffer at pH = 9.0. An aliquot of a freshly-prepared anhydrous DMSO solution of rhodamine (RITC) (10 mg/mL) was added dropwise to the BSA solution at a final fluorophore:protein molar ratio of ca. 10:1. The reaction mixture was kept at room temperature in the dark for 4 hours. The concentration of the fluorescently-labelled proteins was determined by UV-visible spectrophotometry according to the relationship: $[protein] = (A_{280} – w \times A_{max,dye}) / \varepsilon_{protein}$, where $A_{280}$ and $A_{max,\ dye}$ were the absorbances at 280 nm and at the maximum of absorption of the fluorophores respectively (552 nm for RITC), w the correction factor to account for the dye absorption at 280 nm (0.34 for RITC), and $\varepsilon_{protein}$ the extinction coefficient of the BSA (43,824 $cm^{-1}.M^{-1}$). The dye:protein final molar ratio was determined from the ratio $(A_{max,dye}/\varepsilon_{dye}) / ([protein]\ (mg/mL) / M_{protein})$, where ε dye was the molar extinction coefficient of the dyes at their maximum of absorption (65,000 $cm^{-1}.M^{-1}$ for RITC), and $M_{protein}$ the molar mass of the protein (66,430 g/mol for BSA). Typically, the average dye:protein molar ratio was around 1:1. The RITC-BSA stock solution was split into aliquots and stored at -20°C until use.

**Determination of equilibrium partitioning constants and diffusion experiments.**

Three different types of experiments were performed (see details below) to demonstrate (i) the sequestration of three different solutes (calcein, RITC-BSA and SYBR-*ds*DNA) in uncoated dextran-rich droplets, (ii) the retention of solutes within droplets after coating with fatty acid/fatty alcohol bilayers, and (iii) the absence of inward diffusion of the solutes added to the continuous PEG-rich in fatty acid/fatty alcohol-coated dextran-rich droplets. For each experiment, sequestration of SYBR-*ds*DNA, RITC-BSA and calcein into the dextran-rich droplets was monitored by using confocal fluorescence microscopy acquired on a Leica SP2 confocal laser scanning microscope attached to a Leica DMI RE2 inverted microscope using a ×63 oil immersion lens (HCX PL APO, 1.4 NA). The partition constant (K) was determined in each experiment as the ratio of the mean grey fluorescence intensity inside the droplets to that outside the droplets using ImageJ. The average value from 25 droplets from 5 different fields of views of the same sample was reported, together with the associated standard deviation.

(i) Studies on solute partitioning into uncoated dextran-in-PEG solutions were undertaken by adding SYBR-*ds*DNA, RITC-BSA or calcein to a droplets suspension prepared in phosphate buffer (20 mM, pH=10) to obtain final solute concentrations of 0.17 mM, 2.5 µM and 33.5 µM, respectively. The mixture was vortexed just before imaging.

(ii) Studies on solute encapsulation in fatty acid/fatty alcohol-coated dextran-in-PEG droplets were undertaken by adding SYBR-*ds*DNA, RITC-BSA or calcein to a PEG/dextran emulsion under vortexing to reach a final solute concentration of 0.17 mM, 2.5 µM and 33.5 µM, respectively, followed by membrane self-assembly via the dropwise addition of Nile Red-doped sodium oleate then 1-decanol at 5 mM and 15 mM final concentrations, respectively. Note that for RITC-BSA, a Nile Red-free sodium oleate solution was used since Nile Red and RITC fluorescence overlap. Samples were stored in the dark for 24 hours before imaging.

(iii) Studies on diffusion of solutes into fatty acid/fatty alcohol-coated dextran-in-PEG droplets were performed by first adding 2.5 µL of fluorescent solutes (0.5 mM SYBR-*ds*DNA, 7.6 µM RITC-BSA and 100 µM calcein) at one end of a capillary microscopy chamber, followed by the addition of 5 µL of a coated droplets suspension (PEG, 70 mg/mL; dextran, 42.5 mg/mL; sodium oleate, 5 mM and 1-decanol, 15 mM, kept for 24 hours) so that the two solutions mixed together at the contact area. Samples were imaged over ~30 minutes, and time-lapse images acquired every 10 seconds. The final dye concentrations in the microscopy chamber were 0.17 mM, 2.5 µM and 33.5 µM for SYBR-*ds*DNA, RITC-BSA and calcein, respectively. Here again, a Nile Red-free sodium oleate solution for studies involving RITC-BSA was used.

Fluorophores were excited using the following excitation ($\lambda_{ex}$) and emission wavelength range ($\lambda_{em}$); SYBR-*ds*DNA, $\lambda_{ex}$ = 488 nm, $\lambda_{em}$ = 498-517 nm; RITC-BSA, $\lambda_{ex}$ = 543 nm, $\lambda_{em}$ = 555-650 nm; calcein, $\lambda_{ex}$ = 488 nm, $\lambda_{em}$ = 500-540 nm and Nile Red, $\lambda_{ex}$ = 561 nm, $\lambda_{em}$ = 600-750 nm.

**Determination of the CMC of sodium oleate**

The CMC of sodium oleate in phosphate buffer containing or not dextran or PEG was determined using pyrene fluorescence.[35] Briefly, a 0.15 mM stock solution of pyrene fluorescent probe was prepared in ethanol. A series of increasingly concentrated sodium oleate solutions was prepared in phosphate buffer (pH=10.04) in the absence or presence of dextran (42.5 mg/mL) or PEG (70 mg/mL). A small amount of the fluorescent probe was added to each solution (final pyrene concentration of 0.3 µM). Pyrene fluorescence emission spectra were recorded from 350 to 500 nm in 1 nm steps using an excitation wavelength of 340 nm on a Jasco FP-8300 UV-vis spectrofluorometer at 25 °C. The spectra exhibited the characteristic 5 peaks of pyrene fluorescence. The ratio between the fluorescence intensities of the first ($I_{372}$) and third ($I_{392}$) peaks were reported as a function of sodium oleate concentration to determine the CMC as the concentration at which a change in the slope of $I_{372}/I_{392}$ vs. [sodium oleate] was observed. Experiments were repeated three times.

**Zeta potential**

Zeta potential measurements on the different emulsion samples were acquired at t = 0 (i.e. just after formulation and vortexing). Samples were injected into a disposable zeta cuvette and the experiment was run at room temperature using a Malvern Zetasizer (Nano Series) instrument. Three measurements were performed on a same sample, and the average value and standard deviation reported.

**Stabilization of the inverse phase emulsion**

The inverse phase emulsion (PEG-rich droplets suspended in dextran) was prepared as follows. A PEG/dextran stock mixture (20.8 mg/mL PEG, 140 mg/mL dextran) was prepared by dissolving 208 mg of PEG and 1.4 g of dextran in 10 mL of Milli-Q water in a glass container, and mixed under magnetic

stirring for 24 hours at room temperature to ensure complete dissolution of the polymers. This stock solution was stored at 4°C.

To prepare uncoated PEG-in-dextran droplets, 5 µL of FITC-dextran stock solution were added to 2 mL of the stock PEG/dextran solution in an Eppendorf tube and mixed thoroughly by vortexing (final FITC-dextran concentration of 100 nM). To prepare all-aqueous droplets in the presence of amphiphiles, a given volume of Nile Red-doped sodium oleate stock solution was added dropwise to 2 mL of FITC-dextran-doped PEG/dextran mixture in an Eppendorf tube under vortexing (final fatty acid concentration of 8 mM), followed by the dropwise addition of a given volume of pure 1-decanol under vortexing (final decanol concentration of 15 mM).

## Results and discussion

**Interfacial self-assembly of fatty acids in all-aqueous emulsions.**

Direct solubilization and mixing of poly(ethylene glycol) (PEG, $M_w$ = 20 kg/mol, 70 mg/mL) and dextran ($M_w$ = 500 kg/mol, 42.5 mg/mL) in water at room temperature produced an all-aqueous emulsion as a turbid suspension (**Figure 1A**), in agreement with well-established phase diagrams.[36] Confocal fluorescence microscopy images of the suspension doped with fluorescein isothiocyanate-labelled dextran (FITC-dextran, $M_w$ = 500 kg/mol, 100 nM) revealed the presence of polydisperse dextran-rich droplets (typically 20-60 µm in diameter, **Supplementary Figure 2**) showing a homogeneous fluorescent distribution (**Figures 1E** and **Supplementary Figure 3**). The droplets fused together on contact, which rapidly (< 10 min) resulted in macroscopic phase separation into two clear phases, so that a loss of turbidity was observed after 24 hours, with the denser dextran-rich phase sedimenting below the PEG-rich phase (**Figure 1A**). The lower dextran phase was pipetted and imaged again by confocal fluorescence microscopy, which revealed a continuous green fluorescent background without any droplet left (**Figure 1E**). These observations confirmed that the W/W emulsion was not thermodynamically stable.

Sodium oleate (5 mM final concentration > CMC, **Supplementary Figure 4**), a mono-unsaturated fatty acid with 18 carbon atoms, was added under vigorous stirring to the PEG/dextran emulsion in an attempt to stabilize the droplets against coalescence (**Figure 1B**). The pH of the final turbid suspension was 10.6, at which sodium oleate presumably forms micelles[37] (**Supplementary Figure 4**). Confocal fluorescence imaging showed the presence of polydisperse dextran-rich droplets (typically 20-60 µm in diameter, **Supplementary Figure 2**), and revealed that fatty acids (doped with Nile Red) distributed in both the dextran- and PEG-rich phases with a slight propensity to accumulate at the droplets' surface (**Figure 1F** and **Supplementary Figure 3**). A macroscopic phase separation into two clear phases still occurred after 24 hours (**Figures 1B,F**), which indicated that fatty acid micelles and monomers did not allow stabilization of the W/W emulsion.

We then sought to investigate whether oleic acid bilayers would stabilize these all-aqueous emulsions. The simplest approach to produce fatty acid bilayers starting from micelles is to decrease the pH around the acid's pKa.[38 39] Therefore, we first attempted to trigger the formation of oleic acid bilayers around PEG/dextran droplets by decreasing the pH of the emulsion to ~9 using dilute HCl (**Figure 1C**). Confocal fluorescence microscopy of the resulting turbid suspension revealed the presence of more uniform dextran-rich droplets (17.6 ± 5.5 µm, **Supplementary Figure 2**) where Nile Red-doped fatty acids selectively accumulated at the droplets surface (**Figure 1G** and **Supplementary Figure 3**). After 24 hours, the two resulting phases remained turbid but a macroscopic phase separation was observed by eye (**Figure 1C**), and the lower dextran-rich phase did not contain well-defined droplets (**Figure 1G**), indicating that the W/W emulsion was here again unstable against coalescence despite still appearing turbid. This latter observation suggested that turbidity was not a reliable

indicator of stability, which is why we systematically performed microscopy imaging on samples to detect the presence of discrete droplets. We managed to produce a stable emulsion at pH ~ 9 by increasing the sodium oleate concentration to 15 mM. Under these conditions, smaller uniform droplets surrounded by fatty acids were observed (4.6 ± 1.4 µm) and no macroscopic phase separation occurred after 24 hours, confirming that a stable emulsion had formed (**Supplementary Figure 5**).

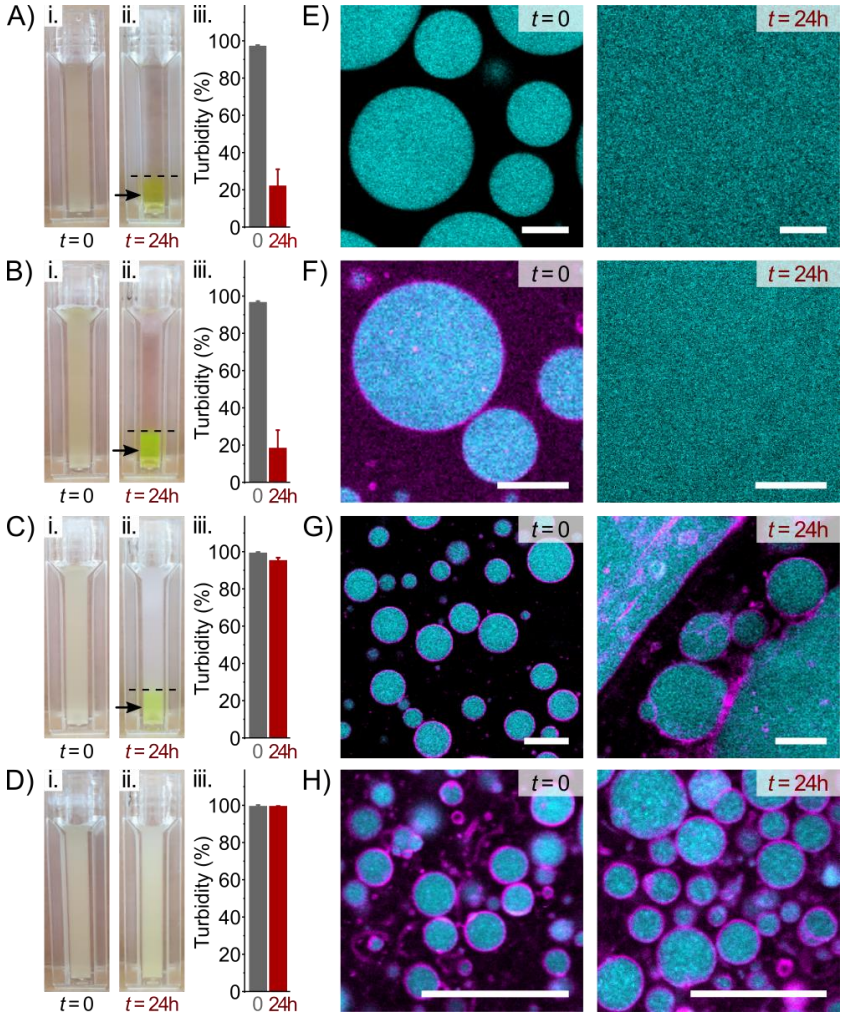


**Figure 1. Interfacial self-assembly of fatty acid onto all-aqueous emulsion droplets.** A-D) Pictures of cuvettes containing PEG/dextran emulsions ([PEG] = 70 mg/mL, [dextran] = 42.5 mg/mL) at *t* = 0 (i) and after 24 hours of resting (ii) prepared in the absence of amphiphiles (A), in the presence of sodium oleate (5 mM) at pH 10.6 (B) or after adjusting the pH to ~9 using HCl (C), or in the presence of both sodium oleate (5 mM) and 1-decanol (15 mM) without altering the pH (D); and corresponding turbidity measured by UV/vis spectroscopy at 700 nm (iii). Error bars represent standard deviations of the average value measured on three different samples. E-H) Confocal fluorescence microscopy images of the same samples as in A-D at *t* = 0 (left) and after 24 hours of resting (right). In the latter case, the bottom of the sample was pipetted and imaged. Droplets and fatty acids are stained with FITC-dextran (100 nM) and Nile Red (1 µM), respectively. False coloring to cyan and magenta were used for FITC-dextran and Nile Red, respectively. Scale bars, 20 µm.

Another well-established approach to obtain fatty acid bilayers is to use admixtures with an alkanol,[38] which produces stable bilayers at lower fatty acid concentration and on a broader pH range. We therefore sought to identify conditions where the addition of alkanol to fatty acid micelles-containing all-aqueous droplets would produce stable W/W emulsions without the need of altering the pH of the solution. Here, 1-decanol was added to a sodium oleate-containing PEG/dextran emulsion under vigorous vortexing (5 mM sodium oleate, 3:1 1-decanol:sodium oleate molar ratio) to produce a highly turbid suspension (**Figure 1D**). The final pH of the solution was 9.9, slightly lower than

in the absence of alkanol. Inspection of the sample with confocal fluorescence microscopy revealed the formation of a few elongated vesicles (**Figure 1H),** confirming that admixtures of sodium oleate and 1-decanol indeed produced bilayers in our concentrated polymer solutions. More importantly, a strong red fluorescence was observed around the green fluorescent, dextran-rich droplets (**Figure 1H** and **Supplementary Figure 3**), suggesting that fatty acids and fatty alcohol accumulated at the PEG/dextran interface. This interfacial accumulation was further supported by the significant decrease of the droplets' zeta potential in the presence of both sodium oleate and 1-decanol (**Supplementary Figure 6**). The average diameter of the resulting droplets was 4.6 ± 1.9 µm (**Figure 2A** and **Supplementary Figure 2**), a size much lower than that observed in the absence of alkanol and/or fatty acids. This decrease in the droplets size pointed to the stabilization of a larger surface area, a characteristic feature of the formation of stable emulsions.[40 41 42] Significantly, the solution remained turbid after 24 hours, and no macroscopic phase separation was observed (**Figures 1D,H**). Confocal fluorescence microscopy images revealed the persistence of uniform droplets that did not exhibit a significant change in size compared to *t* = 0 (4.3 ± 2.0 µm in diameter, **Figure 2A**) and showed red fluorescence only at the interface (**Figure 2B**). Similar observations performed after 3 weeks confirmed that these emulsions remained stable for an extended period of time (**Supplementary Figure 7**). Strikingly, the emulsion could also be centrifuged several minutes at 1500 ×g without fusion of the stabilized droplets (**Supplementary Figure 8**), confirming the formation of a robust membrane that could resist moderate mechanical stress without breaking. In comparison, emulsions prepared without fatty acids and/or without alkanol underwent rapid macroscopic phase separation (**Supplementary Figure 7**), indicating that both sodium oleate and 1-decanol were required for droplet stabilization. Mixtures of sodium oleate and 1-decanol were also efficient in stabilizing an inverse phase system, where PEG-rich droplets were suspended in a dextran-rich phase (see methods), indicating a general fatty acid/fatty alcohol self-assembly mechanism at PEG/dextran interfaces, regardless of the nature of the droplets (**Supplementary Figure 9**).

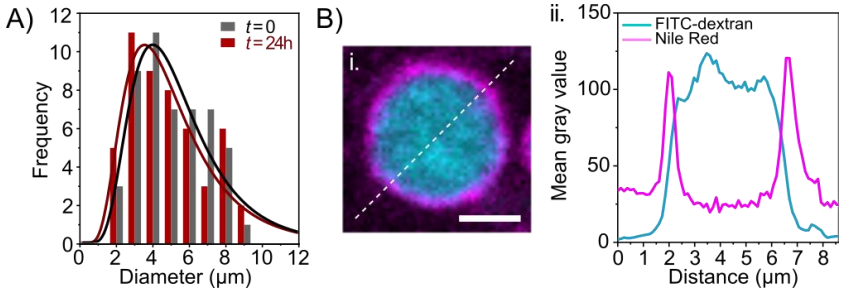


**Figure 2. Fatty acid:fatty alcohol-stabilized all-aqueous emulsions.** A) Distribution in the diameter of dextran-in-PEG droplets produced in the presence of sodium oleate (5 mM) and 1-decanol (15 mM) at *t* = 0 and after 24 hours, showing no change in the average size and polydispersity over time (number of droplets counted: 50). Size distributions were fitted using a log-normal function (shown as solid lines). B) Zoom of a single dextran-rich droplet stabilized by sodium oleate (5 mM) and 1-decanol (15 mM) at *t* = 24h (i) and associated fluorescence intensity line profile (ii, white dashed line in (i)), showing the homogeneous distribution of FITC-dextran throughout the droplet and the selective accumulation of Nile Red-doped fatty acid and fatty alcohol at the interface. False coloring to cyan and magenta were used for FITC-dextran and Nile Red, respectively. Scale bar, 2.5 µm.

**Composition vs. all-aqueous emulsion stabilisation**

The above-discussed stabilized emulsion was obtained with a 3-fold molar excess of 1-decanol compared to sodium oleate. In comparison, mixed alkanol/fatty acid vesicles are typically produced using a much lower fraction of alkanol (~ 1:10 molar ratio).[38 39] We therefore systematically varied the respective amounts of sodium oleate and 1-decanol to evaluate the impact of membrane composition on the stabilization of W/W emulsions. Samples were categorized as unstable when a macroscopic

phase separation was observed by eye after 24 hours, together with the absence of droplets in the lower phase by optical microscopy. Stable emulsions (no macroscopic phase separation) were imaged by optical microscopy and the average size of the droplets measured, which allowed us to build a partial phase diagram (**Figure 3A** and **Supplementary Figure 10**).

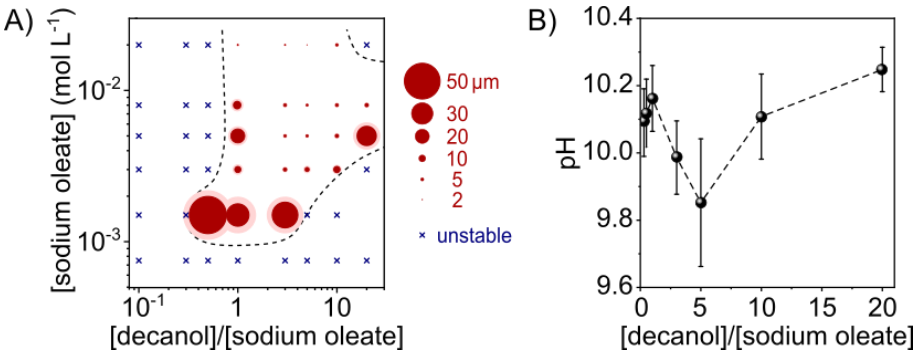


**Figure 3. Lipid composition influences the stability of all-aqueous droplets.** A) Partial phase diagram obtained at different sodium oleate and 1-decanol concentrations, showing the stability domain (dashed black line). Blue crosses mark conditions where macroscopic phase separation is observed after 24 hours. Dark red circles identify conditions where finite-sized droplets persist after 24 hours. The width of the circles is proportional to the diameter of the dextran droplets observed in the samples, as indicated in the legend. Error bars are shown by the light red circles around the dark red circles and represent standard deviations of the average value measured on 50 droplets. B) pH values at t = 0 for dextran-in-PEG droplets prepared at 5 mM sodium oleate for different 1-decanol:sodium oleate molar ratios. Error bars represent standard deviations of the average value measured on three different samples.

Results showed that a critical concentration of sodium oleate and a minimal fraction of 1-decanol were required to produce stable emulsions (**Figure 3A**). At low sodium oleate concentration (0.75 mM), macroscopic phase separation occurred regardless of the amount of 1-decanol added. In contrast, higher sodium oleate concentrations (typically ≥ 5 mM) produced stable emulsions only above a threshold fraction of 1-decanol (typically ≥ 1:1 molar ratio with respect to sodium oleate), but below a critical fraction (< 20:1 alkanol:fatty acid molar ratio). We also measured the pH of samples prepared at varying concentrations of alkanol (**Figure 3B**). Interestingly, we observed that the pH was significantly lower for stable emulsions compared to unstable ones, and the lowest pH were reported for emulsions containing the smallest droplets. A similar trend was observed for all sodium oleate concentrations (**Supplementary Figure 11**), which suggested that there was a correlation between pH variation and the stability of the emulsions.

Overall, these results indicate that low fractions of 1-decanol are unable to produce stable fatty acid bilayers, so that W/W emulsions remain unstable, similarly to emulsions prepared in the presence of sodium oleate micelles or monomers. Above a threshold concentration, 1-decanol favors the formation of fatty acid bilayers stabilized by hydrogen bonds between the two amphiphiles,[38] which results in a change in the fatty acid's pKa (that may account for the change in pH). The necessity to work at an alkanol:fatty acid molar ratio much higher than 1:1, in contrast to what is conventionally used to produce bilayers in pure water, can be attributed to the presence of high concentrations of polymers that may perturb the hydrogen bonding network between the alkanol and the fatty acid, requiring more alkanol to produce fatty acid bilayers.[35, 43] This hypothesis is consistent with the significant shift of the CMC of sodium oleate towards higher values observed in the presence of dextran or PEG (**Supplementary Figure 4**). Finally, at even higher concentrations, 1-decanol phase-separates into oil-rich droplets that partially sequester fatty acid molecules, and that no longer stabilize the W/W emulsions (**Supplementary Figure 12**).

**Structural characterization of the interfacial fatty acid layer**

After establishing the range of lipid composition leading to the stabilization of W/W emulsions, we then sought to better characterize the layer formed around the dextran-rich droplets using freeze-fracture transmission electron microscopy (FF-TEM) combined with small-angle X-ray scattering (SAXS). We chose the W/W emulsion prepared at 5 mM sodium oleate and at a 1-decanol:fatty acid molar ratio equal to 3:1 as our reference sample, where small droplets that persisted in time were produced (**Figures 1D,H**). FF-TEM images revealed that the dextran-rich droplets were coated by multiple uniform layers, each one having an average thickness of 90 ± 20 nm (**Figure 4A**). While such a thickness is too large for a single mixed fatty acid/fatty alcohol bilayer (~ 5 nm),[44] previous studies have reported interlayer spacing values up to ~45 nm in fatty acid multilayers in pure water, which was attributed to the presence of a large water layer between lipid bilayers, partly associated to the electrostatic repulsion between carboxylate anions.[45] The interlayer spacing observed here by FF-TEM is larger than previously reported values, suggesting that the polymers (PEG and dextran) enhance the swelling between bilayers, producing a larger water interlayer.

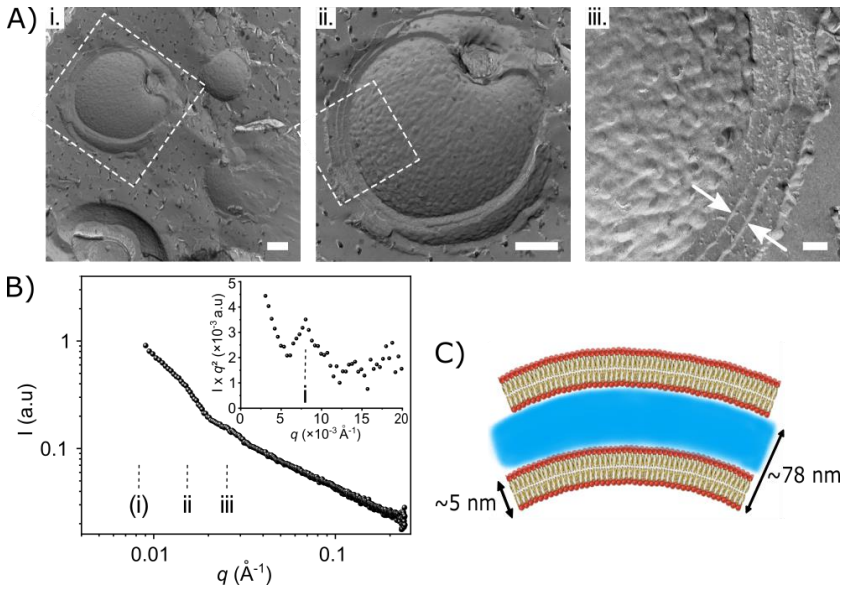


**Figure 4. Interfacial characterization of fatty acid-stabilized droplets.** A) Freeze-Fracture TEM of fatty acid:alkanol-stabilized dextran-rich droplets prepared at 5 mM sodium oleate and 15 mM 1-decanol, showing that droplets are coated by a multilamellar stack of bilayers. Different zooms of the same droplet shown in i. are highlighted in ii. and iii. (white dashed areas). White arrows on image iii. identify one such layer. Scale bars, 500 nm for i-ii and 100 nm for iii. B) 1D SAXS diffractogram of fatty acid:alkanol-stabilized dextran-rich droplets prepared at 5 mM sodium oleate and 15 mM 1-decanol (distance sample-detector: 1.63 m). Inset shows the $I^2$ vs $q$ diffractogram obtained with a different configuration to reach lower $q$ values (distance sample-detector: 2.47 m, see methods). First (i), second (ii) and third (iii) order Bragg reflections are identified on the plots. C) Scheme illustrating the multilamellar stack of bilayers formed at the interface of dextran-in-PEG droplets (please note that for a better visualization the scheme is not to scale).

SAXS measurements performed on a similar sample using two different configurations (i.e., with a distance sample-detector of 1.63 m or 2.47 m, see methods) revealed the existence of three Bragg reflection peaks at $8.1\times10^{-3}$ Å$^{-1}$, $1.6\times10^{-2}$ Å$^{-1}$ and $2.4\times10^{-2}$ Å$^{-1}$ (**Figure 4B**). These peaks were associated to the first, second and third order reflection peaks of a lamellar packing with a repeat distance *d* of 78 nm (see methods), consistent with the FF-TEM observations of a multilamellar structure with a high interlayer spacing. Taken together, FF-TEM and SAXS results point to the formation of polymer-crowded multilamellar giant vesicles (GVs) consisting of sodium oleate:1-decanol bilayers separated by a large water layer (possibly comprising polymers) at PEG/dextran interfaces, as schematically depicted on **Figure 4C**.

**Permeability of crowded fatty acid giant vesicles.**

We last tested the permeability of the fatty acid/fatty alcohol membrane to a range of molecular and macromolecular solutes. A key advantage of W/W emulsions is the ability of the polymer-rich droplets to spontaneously uptake and accumulate solutes based on equilibrium partitioning. Here, we observed by confocal fluorescence microscopy that SYBR Green-labeled double stranded DNA (SYBR-*ds*DNA, ≤ 200 base pairs, 0.17 mM), rhodamine isothiocyanate-labelled BSA (RITC-BSA, $M_W$ = 66,430 g/mol, 2.5 µM) and the molecular dye calcein ($M_W$ = 622 g/mol, 33.3 mM) were all preferentially sequestered within the dextran-rich droplets, with partition coefficients of 2.0 ± 2.4, 1.3 ± 0.3 and 1.3 ± 0.4, respectively (**Figure 5** and **Supplementary Figure 13**). Interestingly, all three solutes were retained within the droplets for at least 24 hours after coating with mixed fatty acid/fatty alcohol bilayers, with different partition coefficients of 1.8 ± 0.4, 14 ± 10 and 1.0 ± 0.3, respectively for SYBR-*ds*DNA, RITC-BSA and calcein (**Figure 5** and **Supplementary Figure 13**). This result indicates that dextran-rich droplets can be used to spontaneously pre-accumulate solutes before the interfacial self-assembly of a membrane, providing a promising strategy to achieve high encapsulation yields in fatty acid-based, polymer-rich giant vesicles.

Even more thrilling, when these fluorescent solutes were added to the W/W emulsion after the fatty acid/alkanol membrane was assembled onto the dextran-rich droplets, the droplets remained dark for at least 30 minutes, and high levels of fluorescence were only observed in the continuous PEG-rich phase (**Figure 5**, **Supplementary Movies 1-3**). The associated partition coefficients of SYBR-*ds*DNA, RITC-BSA and calcein were 0.33 ± 0.1, 0.24 ± 0.07 and 0.04 ± 0.04, respectively, namely well below 1 (**Supplementary Figure 13**). These results indicate that the fatty acid/fatty alcohol multilamellar structure acted as a non-permeable shell around the aqueous droplets, preventing the entry of polynucleotides, proteins, and even low molecular weight molecules on the timescale of the experiment (~30 minutes). Our results are in stark contrast with previous studies reporting the interfacial self-assembly of phospholipids or fatty acids onto polyelectrolyte coacervates, where diffusion of low molecular weight molecules across the membrane was observed.[29 33] Our results therefore suggest that fatty acid/fatty alcohol multilayers produce a defect-free coating on the dextran-rich droplets to make them impermeable even to small solutes, providing a promising strategy to control the diffusion of small molecules in crowded droplets.

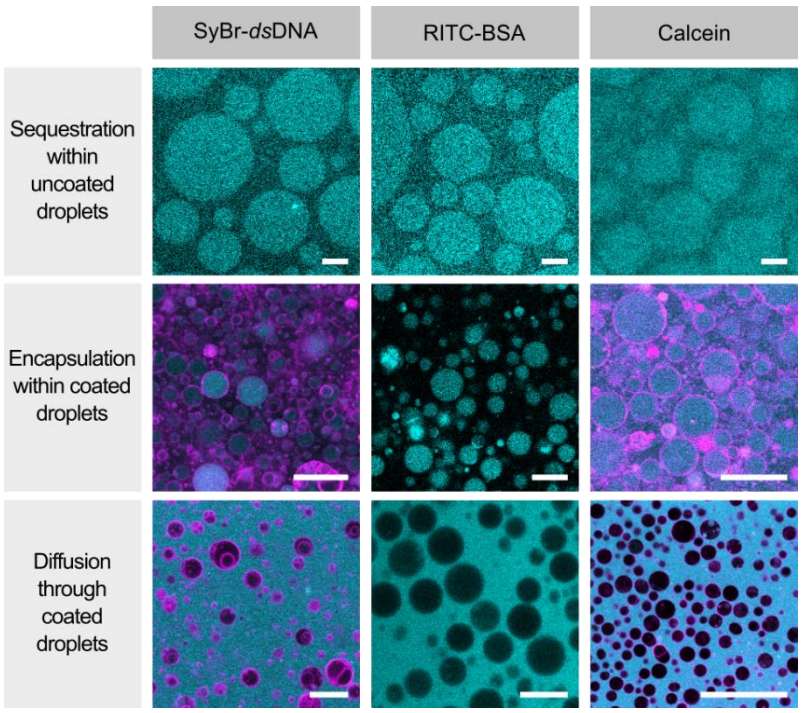


**Figure 5. Permeability of fatty acid membranes assembled on all-aqueous droplets.** Confocal fluorescence microscopy images of the partitioning of SYBR-*ds*DNA (left column), RITC-BSA (middle column) or calcein (right column) in droplets. Top row shows spontaneous sequestration of solutes within uncoated dextran-in-PEG droplets; middle row shows encapsulation of solutes within fatty acid/fatty alcohol-coated droplets (5 mM sodium oleate, 15 mM 1-decanol) after 24 hours; bottom row shows no diffusion of solutes (added to the continuous phase) through fatty acid/fatty alcohol-coated droplets (5 mM sodium oleate, 15 mM 1-decanol) after ~30 minutes. For samples prepared with SYBR-*ds*DNA and calcein, Nile Red was used to label the fatty acid/fatty alcohol bilayer (false coloring to magenta). For the RITC-BSA-containing samples, Nile Red was omitted due to a fluorescence overlap with the RITC dye. False coloring to cyan was used for all three solutes (including for red fluorescent RITC-BSA for consistency). Images show that all three solutes are preferentially partitioned in the dextran-rich phase in the uncoated droplets (top row), and retained inside the coated droplets when added prior to membrane self-assembly (middle row), but do not diffuse through the fatty acid/fatty alcohol membrane when added in the outer phase after membrane self-assembly (bottom row). Scale bars, 20 µm.

## Conclusion

In conclusion, we report the simple formation of stable and impermeable, lipid-coated all-aqueous droplets readily produced by the addition of a fatty acid, sodium oleate, and a short chain alkanol, 1-decanol, to a PEG/dextran emulsion under vigorous mixing.

We hypothesized that sodium oleate and 1-decanol formed a continuous bilayer at the surface of dextran-in-PEG droplets in defined conditions (fatty acid and alkanol concentrations). By combining confocal fluorescence microscopy, small-angle X-ray scattering and freeze-fracture transmission electron microscopy, we validated that lipids spontaneously self-assembled at the surface of dextran-rich droplets to form multilamellar structures, with an interlayer spacing of 78 nm, preventing droplet coalescence, and acting as an impermeable shell that prevented diffusion of oligonucleotides, proteins, but also low molecular weight dyes. We also suggested that the interlayer spacing observed in our work was produced by the swelling between bilayers induced by the presence of polymers (PEG and dextran).

Compared to previous works on the stabilization of complex coacervates or dextran-in-PEG water-in-water emulsions using polymers or lipids, where the membrane was still permeable to small molecules such as glucose[29] but also larger solutes such as oligonucleotides,[33] we here showed that

the formation of multiple fatty acid/alkanol bilayers around the droplets prevented the diffusion of low molecular weight solutes.

Taken together, our results offer a simple procedure to stabilize all-aqueous emulsion droplets capable of encapsulating biomolecules, opening perspectives for the self-assembly of bio-inspired functional artificial cells and greener, solvent-free microencapsulation approaches. Future investigations, e.g., using different fatty acids and polymer concentrations, may help rationalizing what controls the number of bilayers around the aqueous droplets and the interlayer spacing. Interestingly, fatty acids and alkanols are the simplest amphiphiles able to self-assemble into vesicles, and, due to their plausible prebiotic origin, have been extensively used to assemble rudimentary forms of protocells that could have emerged on the early Earth.[38] [46] [47] [48] [49] Our templating strategy could therefore also be a promising approach to produce giant fatty acid protocells able to accumulate material, and study chemical reactions in crowded, confined environments, without loss of droplet integrity.

## CRediT authorship contribution statement

**Noëmie Coudon:** Conceptualization, Methodology, Investigation, Validation, Visualization, Writing – original draft. **Laurence Navailles:** Conceptualization, Methodology, Investigation, Supervision. Writing - review & editing. **Frédéric Nallet:** Conceptualization, Methodology, Investigation. Visualization. Writing - review & editing. **Isabelle Ly:** Methodology, Investigation. **Ahmed Bentaleb:** Methodology, Investigation. **Jean-Paul Chapel:** Conceptualization. Writing - review & editing. **Laure Béven:** Conceptualization. **Jean-Paul Douliez:** Conceptualization, Methodology, Investigation, Supervision, Writing – original draft, Project administration, Funding acquisition. **Nicolas Martin:** Conceptualization, Methodology, Investigation, Visualization, Supervision, Writing – original draft, Project administration.

## Declaration of Competing Interest

The authors declare that they have no known competing financial interests or personal relationships that could have appeared to influence the work reported in this paper.

## Acknowledgments

This work was funded by the French Agence Nationale de la Recherche (ANR-19-CE06-0013-02). N.M. also acknowledges funding from IdEx Bordeaux (ANR-10-IDEX-03-02), an Investissement d'Avenir program of the French government, managed by the Agence Nationale de la Recherche, and from Région Nouvelle-Aquitaine.

## References

[1] C.D. Keating, Aqueous phase separation as a possible route to compartmentalization of biological molecules, Acc. Chem. Res., 45 (2012), 2114-2124

[2] M. Li, X. Huang, T.-Y.D. Tang, S. Mann, Synthetic cellularity based on non-lipid micro-compartments andprotocell models, Curr. Opin. Colloid Int. Sci. 22 (2014), 1-11

[3] B.C. Buddingh, J.C.M. van Hest, Artificial cells: synthetic compartments with life-like functionality and adaptivity, Acc. Chem. Res., 50 (2017), 769-777

[4] N. Martin, Dynamic synthetic cells based on liquid–liquid phase separation, ChemBioChem, 20 (2019), 2553-2568

[5] S. Koga, D.S. Williams, A.W. Perriman, S. Mann, Peptide–nucleotide microdroplets as a steptowards a membrane-free protocell model, Nat. Chem., 3 (2011), 720-724

[6] M. Wang, Y. Wang, Development of surfactant coacervation inaqueous solution, Soft Matter, 10 (2014), 7909-7919

[7] D. Garenne, L. Navailles, F. Nallet, A. Grélard, E.J. Dufourc, J.-P. Douliez, Clouding in fatty acid dispersions for charge-dependent dye extraction, J. Colloid Int. Sci., 468 (2016), 95-102

[8] J.-P. Douliez, N. Martin, C. Gaillard, T. Beneyton, J.-C. Baret, S. Mann, L. Béven, Catanionic coacervate droplets as a surfactant-based membrane-free protocell model, Angew. Chem. Int. Ed., 56 (2017), 13689-13693

[9] M.S. Long, C.D. Jones, M.R. Helfrich, L.K. Mangeney-Savin, C.D. Keating, Dynamic microcompartmentation in synthetic cells, Proc. Natl. Acad. Sci., 102 (2005), 5920-5925

[10] N. Martin, M. Li, S. Mann, Selective uptake and refolding of globular proteins in coacervate microdroplets, Langmuir, 32 (2016), 5881-5889

[11] N. Martin, L. Tian, D. Spencer, A. Coutable-Pennarun, J.L.R. Anderson, S. Mann, Photoswitchable phase separation and oligonucleotide trafficking in DNA coacervate microdroplets, Angew. Chem. Int. Ed., 58 (2019), 14594-14598

[12] T.Z. Jia, C. Hentrich, J.W. Szostak, Rapid RNA exchange in aqueous two-phase system and coacervate droplets, Orig. Life Evol. Biosph., 44 (2014), 1-12

[13] J. Esquena, Water-in-water (W/W) emulsions, Curr. Opin. Colloid Int. Sci., 25 (2016), 109-119

[14] Y.A. Antonov, P. van Puyvelde, P. Moldenaers, Interfacial tension of aqueous biopolymer mixturesclose to the critical point, Int. J. Biol. Macromol. 34 (2004), 29-35

[15] M. Vis, J. Opdam, I.S.J. van't Oor, G. Soligno, R. van Roij, R.H. Tomp, B.H. Erné, Water-in-water emulsions stabilized by nanoplates, ACS Macro Lett., 9 (2015), 965-968

[16] E. Scholten, L.M.C. Sagis, E. van der Linden, Bending rigidity of interfaces in aqueous phase-separated biopolymer mixtures, J. Phys. Chem. B, 108 (2004), 12164-12169

[17] A.T. Poortinga, Microcapsules from self-assembled colloidal particles using aqueous phase-separated polymer solutions, Langmuir, 24 (2008), 1644-1647

[18] T. Nicolai, B. Murray, Particle stabilized water in water emulsions, Food Hydrocolloids, 68 (2017), 157-163

[19] J.-P. Douliez, A. Perro, L. Béven, Stabilization of all-in-water emulsions to form capsules as artificial cells, ChemBioChem, 20 (2019), 2546-2552

[20] J.-P. Douliez, N. Martin, T. Beneyton, J.-C. Eloi, J.-P. Chapel, L. Navailles, J.-C. Baret, S. Mann, L. Béven, Preparation of swellable hydrogel-containing colloidosomes from aqueous two-phase Pickering emulsion droplets, Angew. Chem. Int. Ed., 57 (2018), 7780-7784

[21] S. Zhu, J. Forth, G. Xie, Y. Chao, J. Tian, T.P. Russell, H.C. Shum, Rapid multilevel compartmentalization of stable all-aqueous blastosomes by interfacial aqueous-phase separation, ACS Nano, 14 (2020), 11215-11224

[22] Y. Yin, T. Liu, B. Wang, B. Yin, Y. Yang, T.P. Russell, S. Shi, Nanoparticle/polyelectrolyte complexes for biomimetic constructs, Adv. Funct. Mater., 2108895 (2021)

[23] B.T. Nguyen, W. Wang, B.R. Saunders, L. Benyahia, T. Nicolai, pH-responsive water-in-water Pickering emulsions, Langmuir, 31 (2015), 3605-3611

[24] K.R. Peddireddy, T. Nicolai, L. Benyahia, I. Capron, Stabilization of water-in-water emulsions by nanorods, ACS Macro Letters, 5 (2016), 283-286

[25] A. Gonzalez-Jordan, L. Benyahia, T. Nicolai**,** Influence of the protein particle morphology and partitioning on the behavior of particle-stabilized water-in-water emulsions, Langmuir, 32 (2016), 7189-7197

[26] Y. Song, U. Shimanovich, T.C.T. Michaels, Q. Ma, J. Li, T.P.J. Knowles, H.C. Seum, Fabrication of fibrillosomes from droplets stabilized by protein nanofibrils at all-aqueous interfaces, Nat. Commun., 7 (2016), 12934

[27] F. Dumas, J.-P. Benoit, P. Saulnier, E. Roger, A new method to prepare microparticles based on an aqueous two-phase system (ATPS), without organic solvents, J. Colloid Int. Sci., 599 (2021), 642-649

[28] D.C. Dewey, C.A. Strulson, D.N. Cacace, P.C. Bevilacqua, C.D. Keating, Bioreactor droplets from liposome-stabilized all-aqueous emulsions, Nat. Commun., 5 (2014), 4670

[29] A.F. Mason, B.C. Buddingh, D.S. Williams, J.C.M. van Hest, Hierarchical self-assembly of a copolymer-stabilized coacervate protocell, J. Am. Chem. Soc., 139 (2017), 17309-17312

[30] D.M.A. Buzza, P.D.I. Fletcher, T.K. Georgiou, N. Ghasdian, Water-in-water emulsions based on incompatible polymers and stabilized by triblock copolymers-templated polymersomes, Langmuir, 29 (2013), 14804-14814

[31] T.-Y.D. Tang, R. Che Park, A.J. Thompson, M.K. Kuimova, D.S. Williams, A.W. Perriman, S. Mann, Fatty acid membrane assembly on coacervate microdroplets as a step towards a hybrid protocell model, Nat. Chem., 6 (2014), 527-533

[32] Y. Zhang, Y. Chen, X. Yang, X. He, M. Li, S. Liu, K. Wang, J. Liu, S. Mann, Giant coacervate vesicles as an integrated approach to cytomimetic modeling, J. Am. Chem. Soc., 143 (2021), 2866-2874

[33] F. Pir Cakmak, A.M. Marianelli, C.D. Keating, Phospholipid membrane formation templated by coacervate droplets, Langmuir, 37 (2021), 10366-10375

[34] H. Sakuta, F. Fujita, T. Hamada, M. Hayashi, K. Takiguchi, K. Tsumoto, K. Yoshiwaka, Self-emergent protocells generated in an aqueous solution with binary macromolecules through liquid-liquid phase separation, ChemBioChem, 21 (2020), 3323-3328

[35] M. Delample, F. Jérôme, J. Barrault, J.-P. Douliez, Self-assembly and emulsions of oleic acid–oleate mixtures in glycerol, Green Chem., 13 (2011), 64-68

[36] A.D. Diamond, J.T. Hsu, Phase diagrams for dextran-PEG aqueous two-phase systems at 22°C, Biotechnol. Tech., 3 (1989), 119-124.

[37] K. Suga, D. Kondo, Y. Otsuka, Y. Okamoto, H. Umakoshi, Characterization of aqueous oleic acid/oleate dispersions by fluorescent probes and Raman spectroscopy, Langmuir, 32 (2016), 7606-7612

[38] C.L. Apel, D.W. Deamer, M.N. Mautner, Self-assembled vesicles of monocarboxylic acids and alcohols: conditions for stability and for the encapsulation of biopolymers, Biochim. Biophys. Acta Biomembr., 1559 (2002), 1-9

[39] A. Rendón, D.G. Carton, J. Sot, M. García-Pacios, L.-R. Montes, M. Valle, J.-L.R. Arrondo, F.M. Goñi, K. Ruiz-Mirazo, Model systems of precursor cellular membranes: long-chain alcohols stabilize spontaneously formed oleic acid vesicles, Biophys. J., 102 (2012), 278-286

[40] B. P. Binks, J.A. Rodrigues, Types of phase inversion of silica particle stabilized emulsions containing triglyceride oil, Langmuir, 19 (2003), 4905-4912

[41] S. Arditty, C.P. Whitby, B.P. Binks, V. Schmitt, F. Leal-Calderon, Some general features of limited coalescence in solid-stabilized emulsions, Eur. Phys. J. E, 11 (2003), 273-281

[42] J.M. Montes de Oca-Avalos, R.J. Candal, M.L. Herrera, Nanoemulsions: stability and physical properties, Curr. Opin. Food Sci., 16 (2017), 1-6

[43] O. P. Artykulnyi, V.I. Petrenko, L.A. Bulavin, L. Almasy, N.A. Grigoryeva, M. V. Avdeev, V.L. Aksenov, On the impact of polyethylene glycol on the structure of aqueous micellar solutions of sodium oleate according to small-angle neutron scattering, J. Surf. Investig., 12 (2018), 1142-1148

[44] P. Walde, T. Namani, K. Morigaki, H. Hauser, Formation and properties of fatty acid vesicles (liposomes), Liposome Technol., 1 (2006), 1-19

[45] A.-L. Fameau, F. Cousin, L. Navailles, F. Nallet, F. Boué, J.-P. Douliez, Multiscale structural characterizations of fatty acid multilayered tubes with a temperature-tunable diameter, J. Phys. Chem., 115 (2011), 9033-9039

[46] J.W. Szostak, D.P. Bartel, P.L. Luisi, Synthesizing life, Nature, 409 (2001), 387-390

[47] S.S. Mansy, Model protocells from single-chain lipids, Int. J. Mol. Sci., 10 (2009), 835-843

[48] N. Martin, J.-P. Douliez, Fatty acid vesicles and coacervates as model prebiotic protocells, ChemSystemsChem, 3 (2021), e2100024

[49] R. Rubio-Sanchez, D.K. O'Flaherty, A. Wang, F. Coscia, G. Petris, L. Di Michele, P. Cicuta, C. Bonfio, Thermally driven membrane phase transitions enable content reshuffling in primitive cells, J. Am. Chem. Soc., 143 (2021), 16589-16598.